Data Repository to accompany Tulloch et al.; U-Pb geochronology of Paleozoic plutonism in western New Zealand: implications for S-type granite generation and growth of the east Gondwana margin.

SAMPLED PLUTONS

Plutons are described in an approximate north to south order within the Nelson, Fiordland and Stewart Island blocks.

Nelson Block

Oparara (*quarry*) *granite* is K-feldspar-megacrystic biotite granite typical of much of the northern Karamea Batholith (Rattenbury et al., 1998; Grindley's, (1978) regional 'Karamea Granite'). Aronson (1968) determined Rb-Sr ages of 348 ± 9 on muscovite and 355 ± 9 Ma on biotite from the same site.

Flanagan quartz diorite is equigranular hornblende-biotite quartz diorite. The body is not well mapped, but underlies at least the southern half of a 100nT magnetic anomaly (Reilly, 1970; Tulloch, 1989). Hornblende and biotite K-Ar ages of 162 and 127 Ma have been determined on the same sample (Nathan, et al., 2000).

Domett granite is a medium grained biotite granite from the belt of equigranular granite mapped by Grindley (1978) and Rattenbury et al., (1998; Dke Unit).

Richmond Hill granite. This fine-grained biotite granite (500m x 300m) occurs in tectonic contact with schistose Takaka Terrane metasedimentary rocks (Wilson, 1999). Although grouped with a number of small bodies of fine grained igneous rocks from northwest Nelson (some of which intrude Permian sedimentary rocks) by Grindley (1971) the type locality is characterised by deformational augen, not phenocrysts, and we consider the name *granite* more appropriate than *porphyry*. The small body is significant because of Ag-Pb mineralisation.

Foulwind Granite (Nathan, 1976) outcrops over an area of approximately 3 km^2 at Cape Foulwind. The main phase contains megacrysts of K-feldspar up to 4 cm-long in a medium-coarse (1-10mm) groundmass composed of plagioclase laths set in a matrix of finer grained plagioclase, brown biotite, microcline, quartz and minor muscovite and sporadic coarse, fractured and partly altered Mn-rich garnet. Although plagioclase exhibits only minor deformation of twin lamellae, biotite, microcline and quartz are moderately highly strained and/or partly recrystallised. Zircon, apatite, monazite and less commonly xenotime, are observed as accessory phases. Biotite-rich, hornblende-bearing, granodiorite (Kf1a) with similar chemical characteristics to the granite occurs about 2 km to the south of Cape Foulwind. *Crosscut Granite* is a K-feldspar-megacrystic biotite granite which forms much of the northern Victoria Range (Tulloch, 1979). Intrusive relationships with adjacent Paleozoic plutons have not been observed.

Riwaka Complex (Grindley, 1980) comprises a 8 x 40 km layered lopolith of mafic and ultramafic rocks which intrude Ordovician-Silurian metasedimentary rocks. The dated samples are both from the Brooklyn Diorite which comprises the bulk of the northern part of the Riwaka Complex, and is interpreted as the upper marginal part of the layered intrusion. This unit consists of massive non-cumulate two-pyroxene biotite monzodiorite. Harrison and McDougall, (1980) reported a 367 ± 3 Ma K-Ar hornblende age from the Rameka Gabbro phase to the north. Muir et al., (1996a) reported a significantly older SHRIMP zircon age of 376.9 ± 5.6 Ma on Brooklyn Diorite. P71392 was collected from the outcrop sampled by Muir et al. (1996a) which is ~600 m from surface exposures of an Early Cretaceous phase of the Median Batholith. OU49215 is ~1200m from this Cretaceous pluton.

The Victoria Range segment of the Karamea Batholith (Tulloch, 1979; Rattenbury, 1998) comprises the lower plate of a metamorphic core complex (Tulloch and Challis, 2000) and all rocks yield Mesozoic K-Ar ages. Dated plutons include Crosscut, Tarn Summit, Tobin and Maruia, all of which tend to have granular-polygonal textures and weak-absent zoning in plagioclase.

Tarn Summit Pluton granodiorite is from coarse-grained biotite-rich granodiorite-tonalite orthogneiss covering ~60km^2 in the central Victoria Range.

Maruia Pluton granodiorite comprises biotite-rich granodiorite petrographically similar to Tarn Summit Orthogneiss. The N-S elongate pluton includes abundant metasedimentary inclusions and minor intrusions whose compositions range from diorite to granite.

Tobin Pluton quartz diorite is one of several small hornblende-biotite-(quartz) dioritic plutons up to ~2 km^2 in the Victoria Range. The dated pluton intrudes Tarn Summit Orthogneiss and its eastern margin lies within 500m of a large Early Cretaceous granodiorite intrusion. It includes tonalitic schlieren apparently derived from Tarn Summit Orthogneiss.

Barrytown Granite (Tulloch and Brathwaite, 1986; Laird, 1988, Nathan et al., 2002) is a ~4km^2 pluton of medium grained mostly equigranular biotite granite, zoned (Tulloch, 1986) from a biotite rich rim (sample P45613) to a biotite-poor core (samples P45412, P66549, UC6762 and KF190201-10 are all from the same outcrop at the main road crossing of Granite Creek). *Falls Creek Granite* is similar granite to Barrytown Granite.

Rangitoto granite (Jury, 1981; Cox and Barrell, 2007) is a medium-coarse grained equigranular biotite granite. Barrytown, Falls and Rangitoto plutons all intrude low-grade Greenland Group metasediments.

Kakapotahi granite (Jury, 1981; Cox and Barrell, 2007) is a two-mica medium grained granite containing accessory garnet, fluorite, monazite and xenotime.

Paringa granodiorite forms a ~5 km^2 pluton near the southern end of the Nelson block in south Westland (Mortimer et al., 1984). The hornblende-green biotite granodiorite contains fine grained enclaves of similar mineralogy and is cut by late stage leucogranite dykes. Biotite from the pluton yielded a K-Ar age of 286 Ma (Hurley et al., 1962).

Fiordland Block

Horatio Pluton (Allibone et al. 2009) forms part of the ~80km^2 Seaforth Orthogneiss body of gneissic tonalite-granite in southeastern Fiordland (Gibson, 1982). The medium grained sample dated from Mt Bain comprises gneissic garnetiferous biotite granodiorite.

Dolphin diorite dominates lithologies within the ~30 km^2 Dolphin Intrusive Complex (Ward, 1984), east of the Takaka-Buller terrane boundary (Old Quarry Fault) in Dusky Sound, southwest Fiordland.

Evans Pluton granite is medium grained muscovite (brown) biotite granite which dominates the N-S trending ~20x5 km Evans Pluton (Allibone et al., 2007). The sample exhibits strong ductile deformation/ribboning of quartz, possibly related to Cretaceous detachment faulting.

Newton River Pluton granodiorite is from a ~5x10km coastal exposure of a pluton dominated by coarse-grained K-feldspar megacrystic granodiorite-granite (Allibone et al. 2007). Protomylonitic in places as for nearby Evans Pluton.

Houseroof Pluton tonalite (Allibone et al., 2007; Tine Peak Tonalite of Powell, 2006). Coarse grained, massive to weakly foliated; abundant garnet. Abundant zircon and monazite. Other samples may contain hornblende ± clinopyroxene.

Tower Intrusives comprises 2 N-S trending ~6x1.5km plutons in southern Fiordland. Coarse grained hornblende, clinopyroxene quartz diorite is characterised by abundant garnet (Allibone et al., 2007).

Poteriteri Pluton is ~80km2 pluton of A-type granite in the southern Princes Mountains (Allibone et al. 2009) comprised largely of granite characterised by abundant large squat zircon crystals.

Alice Pluton diorite forms small bodies within the Poteriteri Pluton in the southern Princes Mountains (Allibone et al., 2009).

Big Pluton granite (previously Kakapo Granite). An ~20x15 km pluton on the southern coast. Dominantly granodiorite-granite, minor tonalite. Coarse grained, generally massive, and equigranular-inequigranular, but locally foliated. Accessory garnet, ilmenite, titanite in addition to Ap, Zrn. Intrudes Takaka-Buller Terrane boundary (Allibone et al. 2007).

Ridge Suite granite dike is 3m wide and intrudes Early Paleozoic metasedimentary rocks of Takaka Terrane, north of Big pluton (Allibone et al. 2007).

Stewart Island

Ruggedy Granite is a coarse grained granite extending over a ~ 25x5km belt in northwest Stewart Island (Allibone and Tulloch, 2004). No country rocks are unambiguously recognised (cf. Allibone, 1991). The homogeneous, generally massive and weakly altered granite contains minor clots of green+brown biotite.

Freds Camp Pluton alkali-feldspar granite forms part of several small plutons up to 5x2km within a 30km belt in northeastern Stewart Island (Allibone and Tulloch, 2004). It is extensively intruded by, and faulted against, Mesozoic granites. In the dated sample feldspar is dusty mesoperthite, albite occurs only as blebby grains along K-feldspar rims. Secondary biotite forms clots and some varieties contain blue amphibole and pyroxene.

Ridge tonalite, Table granite and *Knob granite* (Allibone & Tulloch, 1997, 2004) are from gneissic plutons that intrude Pegasus Group metasedimentary rocks of the Takaka Terrane in central Stewart Island. Ridge tonalite is a ~30x1-5 km body of medium-coarse grained inequigranular biotite-rich granodiorite in central Stewart Island. Table granite is a 30 x 1 km sheet of leucogranite intercalated with Ridge tonalite. Knob Granite is from a 10x15 km pluton which is largely surrounded by Early Cretaceous plutons. The dated sample is a coarse-grained muscovite-biotite granite with a ductile fabric of probable Cretaceous age.

ANALYTICAL METHODS

U-Pb laboratory procedures

Zircon, monazite and titanite were separated from the rock samples by standard crushing, heavy liquid, and magnetic separation techniques, and were subsequently hand-picked under a binocular microscope based on clarity and crystal morphology. U-Pb analyses were carried out in three laboratories in the course of this study; San Diego State University, GNS Science (New Zealand) in association with Brown University and, most recently, Massachusetts Institute of Technology (MIT) (Table 2).

Initial analyses were undertaken at the San Diego State University following methods modified from Krogh (1973), using a mixed ^{208}Pb-^{235}U spike and isotopic measurements made on a VG Sector 54 variable multicollector thermal ionization mass spectrometer equipped with a Daly ion counting system for detection of ^{204}Pb (e.g., Kimbrough et al., 1992; 1994). Multi-grain zircon fractions typically weighing 1 to 3 mg were hand picked from mineral separates which had been rinsed with 6.2N HCl and 8N HNO_3. Some zircon fractions were further treated with a mixed HF and HNO_3 solution at ~80°C for 6 to 48 hours in an attempt to remove metamict crystal zones which may have suffered Pb loss (Mattinson, 1994). Replicate analyses of standard zircon OU49127 suggest that typical ^{206}U/^{238}U errors of ~ ± 0.3%, as well as the ^{207}Pb/^{206}Pb errors, calculated using the PBDAT program (Ludwig, 1989) are realistic estimates.

Subsequently, many samples were further analyzed using a spike solution that included ^{205}Pb in order to allow multiple or single grain analyses. Fractions of about 5 to 50 zircon grains were air-abraded (Krogh, 1982) and/or acid-leached prior to dissolution in the GNS/Otago University laboratory in Dunedin by N. Walker utilising a mixed ^{205}Pb-^{235}U-

^{233}U spike. Isotopic measurements were subsequently made by Walker on a Finigan MAT 261 mass spectrometer at Brown University (Getty and Gromet, 1992).
Samples analysed at MIT with few exceptions were single zircon grains. In order to minimize the effects of Pb loss, the grains were pre-treated in one of two ways; conventional mechanical air-abrasion (Krogh, 1982) followed by fluxing in 4N HNO_3 at 80º C, or a version of the thermal annealing and acid leaching (also known as chemical abrasion or CA-TIMS) technique of Mattinson (2005), prior to addition of a mixed ^{205}Pb-^{233}U-^{235}U tracer solution and complete dissolution. Details of zircon pre-treatment, dissolution and U and Pb chemical extraction procedures are described in Ramezani et al. (2007). Pb and U were loaded together onto a single degassed Re filament in a silica-gel/phosphoric acid mixture (Gerstenberger and Haase, 1997) and their isotopic compositions were measured on a VG Sector 54 thermal ionization mass spectrometer. Pb isotopes were measured by peak-hopping using a single Daly photomultiplier detector and U isotopic measurements were made in static mode using multiple Faraday collectors. Mass fractionation for Daly measurements was determined to be 0.25 ± 0.04%/amu over a wide temperature range based on long-term measurements of the NBS-981 Pb standard. U mass fractionation was calculated in real-time using a double spike. All common Pb was attributed to procedural blank. Data reduction, age calculation, and generation of concordia plots were carried out using the algorithms of Ludwig (1980), and the statistical reduction and plotting program ISOPLOT (Ludwig, 2005).

U-Pb data interpretation and error treatment
The U-Pb data presented in this paper were collected in three different laboratories over a period of 16 years, and thus are considerably variable in terms of implemented analytical protocols and precisions of the corresponding data. Our most recent results were produced at MIT and involve analyses of single zircon grains with total radiogenic Pb contents of as little as 3 pg and internal uncertainties of measured dates in the order of 0.1% or better. Furthermore, the application of the CA-TIMS method (Mattinson, 2005) has significantly enhanced the accuracy of U-Pb dates by selectively removing zircon crystal zones prone to radiation damage and Pb loss.

With improved analytical precision, however, additional sources of error that were previously deemed negligible have become significant and must be taken into account. It has now become evident that at high precision even statistically coherent and highly reproducible sets of zircon U-Pb data exhibit slight age discordance manifested by $^{207}Pb/^{206}Pb$ dates that are ~0.2% older than the associated Pb/U dates. This discordance is likely due to imprecision in one or both of the U decay constants (Mattinson, 2000; Schoene et al., 2006) rather than open system behaviour in zircon, and thus limits the application of age concordance (e.g., "Concordia age" of Ludwig, 1998) in the assessment of high-precision U-Pb data. This source of systematic uncertainty is particularly important when isotopic dates measured from different chronometers (e.g., U-Pb and $^{40}Ar/^{39}Ar$) are compared. Another systematic uncertainty of significance is the spike calibration error that must be accounted for when comparison is made between high-precision U-Pb dates produced in different laboratories (i.e., using different spike solutions).

The interpretation of magmatic crystallization ages from U-Pb data involves the choice between multiple isotopic dates, including the $^{206}Pb/^{238}U$, $^{207}Pb/^{206}Pb$ and concordia intercept dates. In general, results from a single, inheritance-free, population of zircons for which Pb loss is non-existent or has been eliminated is represented by a coherent cluster of data (termed "equivalent" by Ludwig, 1998), in which all scatter can be accounted for by analytical uncertainty. In these cases the weighted mean $^{206}Pb/^{238}U$ date of the cluster is considered the most precise and accurate representation of crystallization age. When coherent data sets are not obtainable due to persistent Pb loss that is inferred to have occurred in geologically recent time, we instead rely on the $^{207}Pb/^{206}Pb$ date as the best estimate of the crystallization age. In this case, uncertainties in the decay constants can be generally ignored. If the condition of young-age Pb loss (i.e., lower concordia intercept close to zero) is not satisfied, or zircon inheritance is involved, estimation of the crystallization age will inevitably rely upon the concordia intercept dates. It must be noted that for rocks of Phanerozoic age, the $^{206}Pb/^{238}U$ date is the most sensitive indicator of open-system behaviour (Pb loss and/or inheritance) in zircon.

In order to demonstrate all relevant sources of uncertainty the U-Pb date errors are reported as follows: ±X(Y)[Z] (Table 2), where X is the internal uncertainty in absence of all systematic error (tracer calibration and decay constants), Y includes the tracer calibration error (using a conservative estimate of the 2σ standard deviation of the Pb/U ratio in the tracer to be 0.05%), and Z includes the tracer calibration as well as decay constant errors of Jaffey et al. (1971) (external uncertainty). For $^{207}Pb/^{206}Pb$ dates, tracer errors are negligible and Y is not reported (so it reads ±X[Z]). The MSWD (mean square of the weighted deviates: York, 1967, 1969) of the $^{206}Pb/^{238}U$ weighted mean date is calculated prior to the addition of systematic uncertainties. For the purpose of calculating the duration between two U-Pb ages, we ignore the systematic errors associated with U decay constants as they cancel out (e.g. Bowring et al. 2007). Conservatively, we incorporate the spike U/Pb calibration for durations between samples, including those analysed in the same laboratory.

Oxygen isotopes

Quartz is much less susceptible to alteration than other rock-forming granite minerals and provides a more robust guide to the oxygen isotope ratio of the original magma than whole rock $^{18}O/^{16}O$ ratios (Harris et al., 1997). The $\delta^{18}O$ value for the original magma ($\delta^{18}O$magma) can be estimated from the $\delta^{18}O$ value of the quartz. The $\delta^{18}O$ value of quartz in a granite is dependent on the isotope fractionation between quartz and the melt (Δqtz-magma) and also the cooling rate, which is reflected in the grain-size, and the temperature of closure of the quartz to oxygen diffusion (e.g. Giletti 1986). To correct for the "closure" effects Δqtz-magma for quartz porphyries are assumed to be +1‰ and for coarse–grained granites ≤2‰ (Giletti, 1986; Taylor, 1986). The granites in this study are typically medium grained and so a Δqtz-magma of +1.5‰ is assumed.

Quartz separates were obtained by hand picking using a binocular microscope. In some cases etching of picked minerals by HF vapour was done to ensure purity of quartz. Oxygen was extracted from quartz using laser ablation and BrF5 reagent similar to the procedure described by Sharp (1990). Isotope ratios were determined using a NAA mass spectrometer at GNS Science. The data are reported in the familiar δ notation relative to V-SMOW. Four splits of NBS-28 quartz were run with each batch of 17 quartz samples analysed by laser ablation. Raw sample data were normalised to NBS-28 using a value of 9.64‰ (Coplen, 1983). The average difference between four sets of NBS-28 quartz analyses is 0.16‰.

U-Pb GEOCHRONOLOGIC RESULTS

Samples are discussed in approximate north to south order within western New Zealand (Table DR1). Most monazite analyses reported here display either reverse discordance due to non-equilibrium incorporation of ^{230}Th, and/or significant spread in U-Pb dates due to complex internal age zonation of the monazite grains. Hence ages based exclusively on monazite are of lesser reliability. In general, where sufficient data were not available for calculation of reliable ages, an age approximation has been made (e.g., ~349 Ma), without associated uncertainties, to serve as an indication of possible emplacement age. Caution must be exercised in any interpretation of these approximate ages. In the following discussion of results, interpreted ages have been reported with their total uncertainty incorporating all sources of internal and external error (Z); full error assessment, including a breakdown of various sources of error are given in Table 2. Sample collections: P, PETLAB database (GNS Science, http://pet.gns.cri.nz/); OU, Otago University, Geology Dept.

Nelson Block

Oparara granite, OU50090. All five single-grain zircon CA-TIMS analyses are concordant with uncertainties, though two slightly younger grains probably indicate some degree of Pb loss. The coherent cluster of thee older analyses yields a weighted mean ^{206}Pb/^{238}U date of 370.10 ± 0.67 Ma (MSWD = 0.67), which overlaps within error with the weighted mean ^{207}Pb/^{206}Pb date of all five analyses (371.50 ± 0.94 Ma, MSWD = 0.33).

Flanagan quartz diorite, P45423. Two near-concordant multigrain fractions and one near concordant single grain, and one highly discordant, multi-grain, zircon fraction are interpreted as an inheritance discordia with a lower intercept date of 346.9 ± 1.8 Ma (MSWD = 1.6). Alternatively, the weighted mean ^{206}Pb/^{238}U date of the three near-concordant fractions will be 351.6 ± 2.1 Ma (MSWD = 3.5). However, because of non-negligible scatter in data and discordance, the lower intercept date provides a more meaningful estimate for the crystallization age. The possibility that the three near-concordant fractions are discordant due to Pb-loss is considered unlikely because of the lack of dispersion towards the origin, especially as two of three near concordant fractions were either leached or abraded.

Domett granite, OU50087. Three out of four analyzed multi-grain zircon fractions, including one concordant fraction (>74 µm), yielded ^{207}Pb/^{206}Pb dates that overlap within uncertainty and yield a weighted mean date of 363.1 ± 5.3 Ma (MSWD = 5.2). This date overlaps within error with the $^{206}Pb/^{238}U$ date of the concordant fraction (361.2 ± 1.0 Ma) and serves as the best estimate for the pluton crystallisation age.

Richmond Hill granite, P40375. A coherent cluster of three single-zircon CA-TIMS analyses produced a weighted mean $^{206}Pb/^{238}U$ age of 361.48 ± 0.76 Ma (MSWD = 1.6). A multigrain zircon analysis was highly discordant and younger, but with a comparable $^{207}Pb/^{206}Pb$ date (360.8 Ma) indicating Pb loss.

Riwaka Complex. Two samples from the Brooklyn Diorite have been analyzed. Sample OU49215 was collected 3.1 km SSW of sample P71392. The latter is from an outcrop previously sampled and dated by *in situ* ion microprobe (SHRIMP) U-Pb method (Muir et al., 1996a). These outcrops are located about 1200m and 600m, respectively, from surface exposures of Early Cretaceous plutons in the Median Batholith (Grindley, 1978). Both samples show considerable dispersion in zircon U-Pb dates, but with $^{207}Pb/^{206}Pb$ dates that overlap within uncertainty, indicating variable and persistent Pb loss. For OU49215 the combined weighted mean $^{207}Pb/^{206}Pb$ age of three multi-grain fractions and three GNS single-grain analyses (excluding two reversely discordant analyses) is 364.0 ± 1.1 Ma (MSWD = 1.15). Single zircon grains from sample P71392 were treated by the CA-TIMS technique, except for analysis z9 that was carried out without any pre-treatment. The oldest single-zircon yields a $^{206}Pb/^{238}U$ date of 364.5 Ma which we consider the minimum age for zircon crystallization. Regression of all analyses excluding z1 yields an upper concordia intercept age of 366.5 ± 2.9 Ma (MSWD = 0.04). The weighted mean $^{207}Pb/^{206}Pb$ age of the same group of analyses is 366.3 ± 1.1 Ma (MSWD = 0.04), which is considered to be the best estimate for the age of the rock. All ages for both samples overlap within uncertainties.

Foulwind Granite, OU49201. Four air-abraded zircon and two monazite single crystal analyses produced concordant to near concordant dates between 311 Ma and 319 Ma. Scatter in data in excess of the analytical errors prohibits any reliable age calculation, although the two oldest analyses (z3 and Mz1) alone yield a weighted mean $^{206}Pb/^{238}U$ age of 319.26 ± 0.59 Ma (MSWD = 0.9). We therefore report only an approximate age of ~319 Ma for this intrusion. Younger analyses may reflect a protracted crystallization history or Pb-loss. A multi-grain fraction of coarse zircons yielded a significantly older and discordant date indicating inheritance from a significantly older source. The above date is roughly 8 Ma (2.5%) younger than a SL-13 calibrated SHRIMP age (Muir et al., 1994). Because SL-13 tends to yield ages too young by an average of -1% (Black et al. 2003) the error is likely to be due to beam overlap on inherited cores.

Crosscut Granite, P52241. Two concordant and one older, discordant, single-zircon analyses (air-abraded) yield a lower intercept age of 368.43 ± 0.69 Ma (MSWD = 1.4) and suggest inheritance from a significantly older (Precambrian?) source. Two analyzed monazite fractions have large uncertainties, are reversely discordant and are not suitable for age calculation. Thus, the lower intercept date best represents the pluton emplacement age.

Tarn Summit Tonalite,OU49209. Three air-abraded single zircons and one multi-grain zircon fraction are variably discordant, but fall on a discordia line with a high probability of fit giving a lower concordia intercept date of 369.3 ± 1.8 Ma (MSWD = 0.3) and an upper intercept of ~1186 Ma. A single monazite multigrain fraction with a $^{206}Pb/^{238}U$ age of ~348 Ma is interpreted to reflect a young (Early Cretaceous?) overprint event.

Maruia Granodiorite, P52247. The only analyzed multi-grain zircon fraction (180 µm, L:B 5:1) from this sample is concordant within error, and a pluton crystallisation age of ~345 Ma has been estimated based on its $^{206}Pb/^{238}U$ date.

Tobin quartz-diorite. Four multi-grain zircon fractions from this sample range from concordant to near-concordant. Excluding one analysis with large uncertainty in U-Pb dates, the weighted mean $^{207}Pb/^{206}Pb$ date of the remaining analyses will be 349.7 ± 1.5 Ma (MSWD = 0.56).

Barrytown Granite, P45412. Both inheritance and Pb loss are manifested in the five single-zircon analyses from this sample. However, a coherent cluster of three concordant CA-TIMS analyses yield a weighted mean $^{206}Pb/^{238}U$ age of 368.27 ± 0.57 Ma (MSWD = 0.37). A multi-grain monazite $^{207}Pb/^{235}U$ date of 367.0 ± 3.6 Ma overlaps with the zircon age, as does a biotite K-Ar age of 373 ± 5 Ma (Nathan et al., 2000) and an ion probe U-Pb age of 372.4 ± 5.1 Ma (Muir et al., 1996a).

Falls Creek granite, P45587. Two multi-grain zircon fractions from this sample were variably discordant and different in age. Assuming inheritance as the main source of age discrepancy, a lower concordia intercept date of ~373 Ma can be hypothesized. Two monazite fractions overlap within error but are reversely discordant, indicating the occurrence of excess ^{206}Pb as a result of disequilibrium incorporation of ^{230}Th into monazite. Thus, the $^{206}Pb/^{238}U$ dates are not geologically meaningful. In this case, the weighted mean $^{207}Pb/^{235}U$ age of the monazite analyses (377.3 ± 0.8 Ma) may provide a good estimate for the crystallization age (e.g., Scharer, 1984). We report an approximate pluton age of ~375 Ma based on combined zircon and monazite data.

Kakapotahi granite, P52283. Two monazite fractions overlap in age within uncertainty, but are reversely discordant. As in the case of Falls Creek granite (see above), the weighted mean $^{207}Pb/^{235}U$ age of ~376 Ma provides only an approximation for the pluton crystallization age.

Rangitoto granite, P52355. Seven single-zircon (3 air-abraded and 4 CA-TIMS) analyses from this sample are all concordant within uncertainty, but range in $^{206}Pb/^{238}U$ dates from 368.5 Ma to 370.4 Ma. Age comparison between the air-abraded analyses and the CA-TIMS ones clearly indicates Pb loss that has been more efficiently removed by the annealing-leaching technique. The weighted average $^{206}Pb/^{238}U$ date of the three oldest CA-TIMS zircons is 370.04 ± 0.61 Ma (MSWD = 0.9), which best represents the granite crystallization age.

Paringa granodiorite, OU50100. Five single-zircon CA-TIMS analyses form a coherent cluster with a weighted mean $^{206}Pb/^{238}U$ age of 369.41 ± 0.69 Ma (MSWD = 1.6), which we report as the crystallisation age. The only air-abraded single zircon is distinctly younger indicating the relative inefficiency of the air abrasion technique in removing Pb loss. A multigrain titanite analysis from this sample is distinguishably younger but with a comparable $^{206}Pb/^{207}Pb$ age of ~367.9 Ma, suggesting minor Pb loss.

Fiordland Block

Horatio Pluton, OU49111. A single-zircon analysis from this sample is concordant within uncertainty, whereas a multi-grain fraction is discordant and distinctly younger, though with a comparable $^{207}Pb/^{206}Pb$ date. Assuming Pb loss as the only source of scatter, the weighted mean $^{206}Pb/^{207}Pb$ age of 352.8 ± 2.0 Ma (MSWD = 0.12) is considered the best estimate of the crystallisation age of this rock.

Dolphin diorite, OU49115. Three multi-grain zircon fractions overlap in age within error, one of which is a distinctly younger and less precise analysis. The weighted mean $^{206}Pb/^{238}U$ age of the two older analyses would yield 362.0 ± 1.2 Ma (MSWD = 0.24), although there is not sufficient data to support this calculated age. Alternatively, if zircon inheritance is invoked, regression of the three analyses would yield a lower intercept date of 360.7 ± 2.1 Ma (upper intercept: 1095 ± 590 Ma) with an MSWD of 2.0. The latter provides a more reliable estimate for the crystallization age of the rock.

Evans granite P78948 (Note: renumbered from OU49226 due to double booking of latter number). Two (near-) concordant single-zircon and one highly discordant multi-grain analyses from this sample define a discordia with a lower intercept age of 349.4 ± 1.4 Ma (MSWD = 0.84). This age is consistent with the $^{206}Pb/^{238}U$ date of the most concordant analysis (349.5 Ma), and provides the best estimate for the crystallization age.

Newton River granodiorite, P64999. Both single-zircon analyses from this rock are discordant and do not overlap, except for their $^{207}Pb/^{206}Pb$ dates that yield an imprecise weighted mean date of 349 ± 10 Ma (MSWD = 3.0). Assuming recent Pb loss to be the cause of discordance, an approximate age of ~349 Ma can be inferred for this rock.

Houseroof tonalite, OU58012. Two analyses of multigrain monazite fractions are reversely discordant and only partially overlap, thus not suitable for age calculation. Based on their $^{207}Pb/^{235}U$ dates alone (least affected by disequilibrium incorporation of ^{230}Th in monazite), an approximate age of ~349 Ma is considered for this rock.

Tower Pluton diorite, P73425. The only available analysis from this rock (single-zircon, CA-TIMS) was concordant with a $^{206}Pb/^{238}U$ date of 350.8 ± 0.25 Ma. In the absence of reproducible data, an approximate crystallization age of ~351 Ma is inferred.

Poteriteri Pluton granite, P74751. Three near-concordant single-zircon CA-TIMS analyses from this sample display slight discordance that is positively correlated with age. Regression of all three analyses to a discordia line yields a lower intercept date of

328.7 ± 1.8 Ma (MSWD = 0.11 Ma) which is interpreted as the best estimate for the crystallization age.

Alice diorite, P74756. The crystallization age of this rock is reliably represented by three concordant single-zircon CA-TIMS analyses that overlap in age and constitute a coherent cluster with a weighted mean $^{206}Pb/^{238}U$ date of 340.89 ± 0.65 Ma (MSWD = 0.24).

Big granite, P70787. Six single-zircon CA-TIMS analyses from this rock overlap within error and yield a weighted mean $^{206}Pb/^{238}U$ date of 354.42 ± 0.21 Ma, with a large MSWD of 4.3. This indicates a geologically significant scatter in the data, probably due to slight inheritance or Pb loss. Excluding the oldest analysis (z4) as an outlier (affected by inheritance), the remaining five analyses give a more statistically valid weighted mean date of 354.35 ± 0.58 Ma (MSWD = 1.3). The sixth analysis has a slightly older $^{206}Pb/^{238}U$ age of 354.8 Ma suggestive of a trace of the inheritance. The latter probably explains older *in situ* (SHRIMP) U-Pb ages obtained by Muir et al. (1998).

Ridge Suite granite dike, P71266. Two single-zircon CA-TIMS analyses do not overlap, with one displaying reverse discordance. No reliable age can be calculated. However, based on the $^{207}Pb/^{206}Pb$ dates of the available analyses and the assumption of Pb loss, an approximate age of ~351 Ma is inferred for this rock.

George Sound granites. Bradshaw and Kimbrough (1991) reported a mid-Paleozoic age for mainly A-type granitoid enclaves within Early Cretaceous Western Fiordland Orthogneiss at George Sound. We note that five of six (excluding OU 51837) $^{207}Pb/^{206}Pb$ ages are close to 310 Ma, which we consider a more likely emplacement age for these three rocks.

Stewart Island

Ruggedy Granite, P62175. Two single-zircon analyses overlap within error and are concordant, with a weighted mean $^{206}Pb/^{238}U$ date of ~342 Ma. Three multi-grain zircon analyses from this sample gave younger $^{206}Pb/^{238}U$ dates (333.2 to 335.5 Ma) but $^{207}Pb/^{206}Pb$ dates that overlap with those of single-grain analyses. The weighted mean $^{207}Pb/^{206}Pb$ date of all five analyses is 341.5 ± 4.2 Ma (MSWD = 0.21), which provides the best estimate for crystallization age of the granite.

Freds Camp Alkali-feldspar granite, P57426. Four single-zircon CA-TIMS analyses define a coherent cluster with a weighted mean $^{206}Pb/^{238}U$ date of 305.69 ± 0.50 Ma (MSWD = 1.13). A three-grain zircon analysis from another sample of this pluton (P58515) is discordant indicating significant Pb-loss, but its $^{207}Pb/^{206}Pb$ date of 307.6 ± 0.9 Ma is in perfect agreement with the $^{207}Pb/^{206}Pb$ dates of the four single analyses.

Ridge tonalite, P57323. The single-zircon (3 abraded and 2 CA-TIMS) analyses of this sample are mostly plagued by inheritance from variable old-age sources. However, the two youngest data points combined with a multi-grain zircon analysis fall on a discordia with a lower intercept date of 345.2 ± 5.0 Ma (MSWD = 1.2), which we interpret as the magmatic crystallization age.

Table granite, P60678. The only two single-zircon analyses from this sample are variably discordant and different in age. Assuming a simple Pb loss model, a hypothetical discordia line passing through the analyses would yield an upper intercept date of ~340 Ma, which we infer as an approximation for the crystallization age. The lower intercept age of ~126 Ma is consistent with the subsequent intrusion and enclosure of this unit by several Early Cretaceous plutons (Allibone and Tulloch, 2004).

Knob Granite, P63648. A single-grain and a multi-grain monazite fraction have comparable $^{207}Pb/^{206}Pb$ dates with a weighted mean date of 305 ± 2 Ma. Considering the possibility of presence of excess ^{206}Pb in monazite due to Th disequilibrium effects, this should be considered a minimum age for Knob Granite crystallisation. A hypothetical discordia line anchored at 80 Ma, the age of ductile deformation of this rock (timing of monazite recrystallisation and/or Pb loss) within the Sisters Shear Zone (Kula et al., 2007), would yield an upper intercept date of 316.6 ± 6.2 Ma.

Marie Byrd Land - S-type granites in West Antarctica
New Zealand and West Antarctica formed contiguous sectors within the Pacific margin of Gondwana prior to Late Cretaceous breakup (e.g., Eagles et al., 2004). Monazite $^{207}Pb/^{235}U$ ages from two samples from West Antarctica suggest minimum ages of ~351 and 359 Ma for 2-mica granites from Neptune Nunatak and the Chester Mountains, respectively (Fig. DR1).

Chester Mountains. Two monazite fractions are reversely discordant. The oldest fraction has a $^{207}Pb/^{235}U$ age of 359.1 ± 1.6 Ma and we report ~359 Ma as a minimum pluton crystallisation age.
Neptune Nunatak. Two monazite fractions exhibit normal discordance with an upper intercept age of 351 ± 16 Ma from which we report ~351 Ma as a minimum pluton crystallisation age.

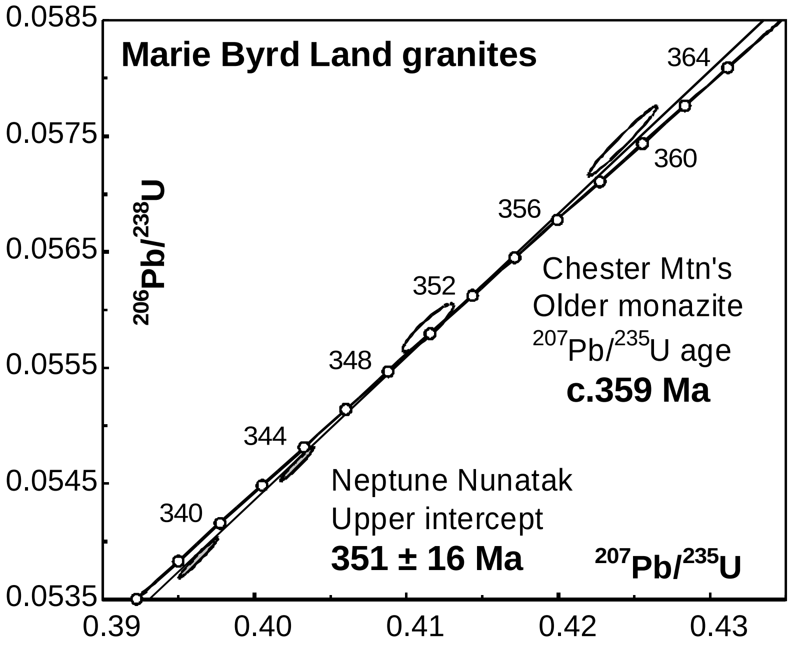

Fig. DR1. Monazite U-Pb ages from the Chester Mountains and Neptune Nunatak of Marie Byrd Land.

DISCUSSION OF S-TYPE CHARACTER OF KARAMEA SUITE

Muir et al. (1996b) confused the batholith-suite concepts outlined by Tulloch (1988) when they misquoted Cooper and Tulloch (1992): " .... the Karamea *Batholith* (sic) .... is distinctly S-type in character". Muir et al. also noted that some samples (from the Karamea Batholith) were ambiguous in terms of the I-S granite classification with respect to Chappell and White (1974, 1992) criteria such as ASI, Sri etc. However, Muir et al.'s samples have lower ASI indices for plutons common to both sample sets (e.g., Muir et al., 1996b Barrytown sample BA has a lower ASI index than all 12 of our Barrytown analyses), and their samples extend to somewhat higher Na (and thus possibly a higher ASI index) than our set. One explanation for the difference may be due to their analysis of undated samples that may be of very different age (e.g., Britannia Granite, some of which is Cretaceous; O'Sullivans Granite sample RNZ 271). Regardless, none of Muir's samples (excluding RNZ 271 and the mafic rocks of the Riwaka Complex and Mt Zetland) have ASI indices less than Chappell and Whites (1992) S-type boundary of value of 1.056. Nor are any of Muir's initial $^{87}Sr/^{86}Sr$ values less than the (Lachlan) S-type field when they are recalculated at 370 Ma (cf. 380, not 375 Ma), yielding initial Sr values higher by ~ 0.001-0.002 than reported (see Fig 12).

REFERENCES CITED

Allibone, A. H., 1991, Volcanogenic and granitoid rocks from Northwest Stewart Island: New Zealand Journal of Geology and Geophysics, v. 34, no. 1, p. 35-50.

Allibone, A. H., and Tulloch, A. J., 1997, Metasedimentary, granitoid, and gabbroic rocks from central Stewart Island, New Zealand: New Zealand Journal of Geology and Geophysics, v. 40, no. 1, p. 53-68.

-, 2004, Geology of the plutonic basement rocks of Stewart Island, New Zealand: New Zealand Journal of Geology and Geophysics, v. 47, no. 2, p. 233-256.

Allibone, A. H., Turnbull, I. M., Tulloch, A. J., and Cooper, A. F., 2007, Plutonic rocks of the Median Batholith in southwest Fiordland, New Zealand: field relations, geochemistry, and correlation: New Zealand Journal of Geology and Geophysics, v. 50, no. 4, p. 283–314.

-, 1968, Regional geochronology of New Zealand: Geochimica et Cosmochimica Acta, v. 32, no. 7, p. 669-697.

Black, L. P., Kamo, S. L., Williams, I. S., Mundil, R., Davis, D. W., Korsch, R. J., and Foudoulis, C., 2003, The application of SHRIMP to Phanerozoic geochronology; a critical appraisal of four zircon standards: Chemical Geology, v. 200, no. 1-2, p. 171-188.

Bowring, S. A., Grotzinger, J. P., Condon, D. J., Ramezani, J., Newall, M., and Allen, P. A., 2007, Geochronologic constraints of the chronostratigraphic framework of the Neoproterozoic Huqf Supergroup, Sultanate of Oman: American Journal of Science, v. 307, no. 10, p. 1097-1145.

Bradshaw, J. D., and Kimbrough, D. L., 1991, Mid-Paleozoic age of granitoids in enclaves within Early Cretaceous granulites, Fiordland, southwest New Zealand: New Zealand Journal of Geology and Geophysics, v. 34, no. 4, p. 455-469.

Chappell, B. W., and White, A. J. R., 1974, Two contrasting granite types: Pacific Geology, v. 8, Circum-Pacific plutonism, p. 173-174.

-, 1992, I- and S-type granites in the Lachlan fold belt, *in* Brown, P. E., and Chappell, B. W., eds., The second Hutton symposium on the Origin of granites and related rocks: Special Paper - Geological Society of America: Canberra, Australia, p. 1-26.

Cooper, R. A., and Tulloch, A. J., 1992, Early Palaeozoic terranes in New Zealand and their relationship to the Lachlan fold belt: Tectonophysics, v. 214, no. 1-4, p. 129-144.

Coplen, T. B., Kendall, C., and Hopple, J., 1983, Comparison of stable isotope reference samples: Nature (London), v. 302, no. 5905, p. 236-238.

Cox, S. C., and Barrell, D. J. A., 2007, Geology of the Aoraki area, QM15: GNS Science, Lower Hutt, New Zealand, scale 1:250,000.

Eagles, G., Gohl, K., and Larter, R. D., 2004, High-resolution animated tectonic reconstruction of the South Pacific and West Antarctic margin: Geochemistry, Geophysics, Geosystems - G^3, v. 5, no. 7, p. 21.

Gerstenberger, H., and Haase, G., 1997, A highly effective emitter substance for mass spectrometric Pb isotope ratio determinations: Chemical Geology, v. 136, no. 3-4, p. 309-312.

Getty, S. R., and Gromet, L. P., 1992, Geochronological constraints on ductile deformation, crustal extension, and doming about a basement-cover boundary, New England Appalachians: American Journal of Science, v. 292, no. 6, p. 359-397.

Gibson, G. M., 1982, Stratigraphy and petrography of some metasediments and associated intrusive rocks from central Fiordland, New Zealand: New Zealand Journal of Geology and Geophysics, v. 25, no. 1, p. 21-43.

Giletti, B. J., 1986, Diffusion effects on oxygen isotope temperatures of slowly cooled igneous and metamorphic rocks: Earth and Planetary Science Letters, v. 77, no. 2, p. 218-228.

Grindley, G. W., 1971, Geological map of New Zealand; sheet S8, Takaka (ed. 1): Department of Scientific and Industrial Research, Wellington, New Zealand, scale 1:63,360.

-, 1978, West Nelson, *in* Suggate, R. P., Stevens, G. R., and Te Punga, M. T., eds., The Geology of New Zealand, New Zealand Geological Survey, Lower Hutt, New Zealand, p. 96-99.

Harris, C., Faure, K., Diamond, R. E., and Scheepers, R., 1997, Oxygen and hydrogen isotope geochemistry of S- and I-type granitoids; the Cape Granite Suite, South Africa: Chemical Geology, v. 143, no. 1-2, p. 95-114.

Harrison, T. M., and McDougall, I., 1980, Investigations of an intrusive contact, Northwest Nelson, New Zealand; I, Thermal, chronological and isotopic constraints: Geochimica et Cosmochimica Acta, v. 44, no. 12, p. 1985-2004.

Hurley, P. M., Fairbairn, H. W., Hughes, H., and Pinson, W. H., Jr., 1962, Radiogenic argon and strontium diffusion parameters in biotite at low temperatures obtained

from Alpine fault uplift in New Zealand: Geochimica et Cosmochimica Acta, v. 26, p. 67-80.
Jaffey, A. H., Flynn, K. F., Glendenin, L. E., Bentley, W. C., and Essling, A. M., 1971, Precision Measurement of Half-Lives and Specific Activities of 235U and 238U: Physical Review C, v. 4, no. 5, p. 1889-1906.
Jury, A. P., 1981, Mineralization at Mt Rangitoto and Mt Greenland, Westland [M.Sc. thesis]: University of Canterbury, Christchurch, New Zealand, 124 p.
Kimbrough, D. L., Mattinson, J. M., Coombs, D. S., Landis, C. A., and Johnston, M. R., 1992, Uranium-lead ages from the Dun Mountain ophiolite belt and Brook Street Terrane, South Island, New Zealand: Geological Society of America Bulletin, v. 104, no. 4, p. 429-443.
Kimbrough, D. L., Tulloch, A. J., Coombs, D. S., Landis, C. A., Johnston, M. R., and Mattinson, J. M., 1994, Uranium-lead zircon ages from the Median Tectonic Zone, South Island, New Zealand: New Zealand Journal of Geology and Geophysics, v. 37, no. 4, p. 393-419.
Krogh, T. E., 1973, A low-contamination method for hydrothermal decomposition of zircon and extraction of U and Pb for isotopic age determinations: Geochimica et Cosmochimica Acta, v. 37, no. 3, p. 485-494.
-, 1982, Improved accuracy of U-Pb zircon ages by the creation of more concordant systems using an air abrasion technique: Geochimica et Cosmochimica Acta, v. 46, no. 4, p. 637-649.
Kula, J., Tulloch, A., Spell, T. L., and Wells, M. L., 2007, Two-stage rifting of Zealandia-Australia-Antarctica; evidence from $^{40}Ar/^{39}Ar$ thermochronometry of the Sisters shear zone, Stewart Island, New Zealand: Geology (Boulder), v. 35, no. 5, p. 411-414.
Laird, M. G., 1988, Geological Map of New Zealand; Sheet S37, Punakaiki: Department of Scientific and Industrial Research, Wellington, New Zealand, scale 1:63,360.
Ludwig, K.L., 1989, PBDAT for MS-DOS, a computer program for IBM PC compatibles for processing raw U-Th-Pb isotope data, version 1.05, revised April 1989, United States Geological Survey, 88-542 p.
-, 1980, Calculation of uncertainties of U-Pb isotope data: Earth and Planetary Science Letters, v. 46, no. 2, p. 212-220.
-, 1998, On the treatment of concordant uranium-lead ages: Geochimica et Cosmochimica Acta, v. 62, no. 4, p. 665-676.
-, 2005, Isoplot 3.00; A geochronological toolkit for Microsoft Excel: Berkeley Geochronology Center Special Publication No. 4.
Mattinson, J. M., 1994, A study of complex discordance in zircons using step-wise dissolution techniques: Contributions to Mineralogy and Petrology, v. 116, no. 1-2, p. 117-129.
-, 2000, Revising the ‘‘gold standard’’—the uranium decay constants of Jaffey et al., 1971.: Eos, Transactions, American Geophysical Union, Spring Meeting Supplement, Abstract V61A-02, p. S444-S445.
-, 2005, Zircon U/Pb chemical abrasion (CA-TIMS) method; combined annealing and multi-step partial dissolution analysis for improved precision and accuracy of zircon ages: Chemical Geology, v. 220, no. 1-2, p. 47-66.
Mortimer, G., Nathan, S., Dawson, R. M., and Eggers, M. J., 1984, Geology of the

lowland area between the Cook and Paringa rivers, South Westland: New Zealand Geological Survey Report 81, 49 pages.
Muir, R. J., Ireland, T. R., Weaver, S. D., and Bradshaw, J. D., 1994, Ion microprobe U-Pb zircon geochronology of granitic magmatism in the Western Province of the South Island, New Zealand: Chemical Geology, v. 113, no. 1-2, p. 171-189.
-, 1996, Ion microprobe dating of Paleozoic granitoids; Devonian magmatism in New Zealand and correlations with Australia and Antarctica: Chemical Geology, v. 127, no. 1-3, p. 191-210.
Muir, R. J., Weaver, S. D., Bradshaw, J. D., Eby, G. N., Evans, J. A., and Ireland, T. R., 1996, Geochemistry of the Karamea Batholith, New Zealand and comparisons with the Lachlan fold belt granites of SE Australia: Lithos, v. 39, no. 1-2, p. 1-20.
Muir, R. J., Ireland, T. R., Weaver, S. D., Bradshaw, J. D., Evans, J. A., Eby, G. N., and Shelley, D., 1998, Geochronology and geochemistry of a Mesozoic magmatic arc system, Fiordland, New Zealand: Journal of the Geological Society of London, v. 155, Part 6, p. 1037-1053.
Nathan, S., 1976, Geological map of New Zealand; Sheets S23/9 and S24/7, Foulwind and Westport: Department of Scientific and Industrial Research, Wellington, New Zealand, scale 1:25,000.
Nathan, S., Rattenbury, M. S., and Suggate, R. P., 2002, Geology of the Greymouth area: Institute of Geological and Nuclear Sciences, Lower Hutt, New Zealand, scale 1:250,000.
Nathan, S., Thurlow, C., Warnes, P., and Zucchetto, R., 2000, Geochronology database for New Zealand rocks; 1961-1999: Institute of Geological and Nuclear Sciences Science Report 2000/11, 51 pages.
Powell, N.G., 2006, The geology of central southern Fiordland, with emphasis on the cause of polybaric Cretaceous metamorphism in western New Zealand [Ph.D. thesis]: University of Otago, Dunedin, New Zealand, 344 p.
Ramezani, J., Schmitz, M. D., Davydov, V. I., Bowring, S. A., Snyder, W. S., and Northrup, C. J., 2007, High-precision U-Pb zircon age constraints on the Carboniferous-Permian boundary in the southern Urals stratotype: Earth and Planetary Science Letters, v. 256, no. 1-2, p. 244-257.
Rattenbury, M. S., A., C. R., and Johnston, M. R., 1998, Geology of the Nelson area, QM9: Institute of Geological and Nuclear Sciences, Lower Hutt, New Zealand, scale 1:250,000
Reilly, W. I., 1970, Magnetic Map of New Zealand; Buller, total force anomalies: Department of Scientific and Industrial Research, Wellington, New Zealand, scale 1:250,000.
Scharer, U., 1984, The effect of initial ^{230}Th disequilibrium on young U-Pb ages; the Makalu case, Himalaya: Earth and Planetary Science Letters, v. 67, no. 2, p. 191-204.
Schoene, B., Crowley, J. L., Condon, D. J., Schmitz, M. D., and Bowring, S. A., 2006, Reassessing the uranium decay constants for geochronology using ID-TIMS U–Pb data: Geochimica et Cosmochimica Acta, v. 70, p. 426-445.
Sharp, Z. D., 1990, A laser-based microanalytical method for the in situ determination of oxygen isotope ratios of silicates and oxides: Geochimica et Cosmochimica Acta, v. 54, no. 5, p. 1353-1357.

Stacey, J. S., and Kramers, J. D., 1975, Approximation of terrestrial lead isotope evolution by a two-stage model: Earth and Planetary Science Letters, v. 26, no. 2, p. 207-221.
Steiger, R. H., and Jaeger, E., 1977, Subcommission on geochronology; convention on the use of decay constants in geo- and cosmochronology: Earth and Planetary Science Letters, v. 36, no. 3, p. 359-362.
Taylor, H. P., Jr., and Sheppard, S. M. F., 1986, Igneous rocks; I, Processes of isotopic fractionation and isotope systematics, *in* Valley, J. W., Taylor, H. P., Jr, and O'Neil, J. R., eds., Stable Isotopes in high temperature processes: Reviews in Mineralogy volume 16, Mineralogical Society of America, p. 227-271.
Tulloch, A. J., 1979, Plutonic and metamorphic rocks in the Victoria Range segment of the Karamea Batholith [Ph.D. thesis]: University of Otago, Dunedin, New Zealand, 301 p.
-, 1986, Hydrothermal alteration and scheelite mineralization associated with the Barrytown Pluton, North Westland, New Zealand: Mineral Deposits (Kuangchuang Dizhi), v. 5, no. 3, p. 27-36.
-, 1988, Batholiths, plutons, and suites; nomenclature for granitoid rocks of Westland-Nelson, New Zealand: New Zealand Journal of Geology and Geophysics, v. 31, no. 4, p. 505-509.
-, 1989, Magnetic susceptibilities of Westland-Nelson plutonic rocks; discrimination of Paleozoic and Mesozoic granitoid suites: New Zealand Journal of Geology and Geophysics, v. 32, no. 2, p. 197-203.
Tulloch, A. J., and Brathwaite, R. L., 1986, C7; Granitoid rocks and associated mineralisation of Westland - West Nelson: Record - New Zealand Geological Survey, v. 13, p. 65-92.
Tulloch, A. J., and Challis, G. A., 2000, Emplacement depths of Paleozoic-Mesozoic plutons from western New Zealand estimated by hornblende-Al geobarometry: New Zealand Journal of Geology and Geophysics, v. 43, no. 4, p. 555-567.
Ward, C. M., 1984, Geology of the Dusky Sound area, Fiordland, with emphasis on the structural-metamorphic development of some pyroblastic staurolite pelites [Ph.D. thesis]: University of Otago, Dunedin, New Zealand, 353 p.
Wilson, E., 1999, Geology of the lower Parapara River [MSc thesis]: Victoria University of Wellington, Wellington, New Zealand.
York, D., 1967, The best isochron: Earth and Planetary Science Letters, v. 2, no. 5, p. 479-482.
-, 1969, Least squares fitting of a straight line with correlated errors: Earth and Planetary Science Letters, v. 5, no. 5, p. 320-324.

Table DR1. U-Pb data for Paleozoic plutons of western New Zealand and West Antarctica

Sample No.	Fraction, mineral, pretreatment	Weight (mg)	Concentrations U (ppm)	Concentrations Pb (ppm)	Pb(c) (pg)	Pb (rad) / Pb(c)	Th / U	208 Pb / 206 Pb	206 Pb / 204 Pb	Radiogenic ratios 207 Pb / 235 U	err (2s%)	206 Pb / 238 U	err (2s%)	corr. coef.	207 Pb / 206 Pb	err (2s%)	Age (Ma) 206 Pb / 238 U	207 Pb / 235 U	207 Pb / 206 Pb
Nelson block																			
Oparara	z1 AnLh**				1.0	83.5	0.36	0.113	5266	0.4391	0.09	0.05897	0.06	0.647	0.054011	0.07	369.33	369.63	371.5
OU50090	z2 AnLh**				1.04	54.21	0.28	0.088	3499	0.4403	0.18	0.05911	0.14	0.769	0.054015	0.12	370.23	370.43	371.7
	z3 AnLh**				1.1	84.5	0.22	0.068	5541	0.4391	0.13	0.05896	0.08	0.637	0.054010	0.10	369.29	369.59	371.5
	z4 AnLh**				0.5	292.2	0.16	0.050	19429	0.4405	0.16	0.05911	0.09	0.583	0.054041	0.13	370.22	370.57	372.8
	z5 AnLh**				0.6	164.4	0.18	0.058	10865	0.4398	0.11	0.05908	0.06	0.553	0.053992	0.09	370.02	370.12	370.7
	>150um sp Lh	2.400	165	11					20150	0.6183	0.28	0.06985	0.27	0.96	0.064202	0.08	435.2	488.8	748.3
Flanagan	200um, 2:1, Ab, 22gr*	0.08	280	18					11023	0.5491	0.22	0.06470	0.21	0.95	0.615580	0.00	404.2	444.5	658.8
P45423	175um, 5:1, Lh, 21gr*	0.090	247	15					4687	0.4174	0.26	0.05597	0.21	0.84	0.054085	0.00	351.1	354.2	374.6
	125um, 5:1, 20gr*	0.120	144	14					108	0.4202	1.00	0.05627	0.32	0.48	0.054158	0.89	352.9	356.2	377.6
	140um, 3:1, 13gr**	0.008	269	20					200	0.4208	0.67	0.05606	0.26	0.49	0.054440	0.59	351.6	356.6	389.2
Domett	<74um	3.500	1348	78					5376	0.4242	0.28	0.05714	0.27	0.97	0.053843	0.06	358.2	359.1	364.5
OU50087	>74um	3.500	458	27					3307	0.4272	0.29	0.05764	0.27	0.96	0.053752	0.08	361.2	361.2	360.7
	<74um Lh	4.900	426	25					4296	0.4263	0.30	0.05746	0.28	0.96	0.053810	0.08	360.2	360.6	363.0
	>74um Lh	4.8	195	11					15175	0.4291	0.29	0.05745	0.27	0.96	0.054170	0.08	360.1	362.5	378.0
Richmond	z2 AnLh**				0.5	87.5	0.41	0.128	5445	0.4280	0.09	0.05769	0.06	0.60	0.053806	0.08	361.59	361.77	362.9
P40375	z3 AnLh**				0.4	118.7	0.37	0.118	7448	0.4278	0.10	0.05768	0.06	0.54	0.053785	0.09	361.51	361.59	362.1
	z1 AnLh**				0.4	148.6	0.34	0.106	9413	0.4276	0.09	0.05766	0.05	0.62	0.053789	0.07	361.35	361.47	362.2
	bulk Lh	1.50	17	345					31323.7	0.3742	0.28	0.05049	0.27	0.98	0.053755	0.05	317.54	322.79	360.81
Riwaka	cg	22.100	173	11					2151	0.4311	0.40	0.05808	0.34	0.86	0.053830	0.21	364.0	364.0	364.0
OU49215	>250um Lh	3.600	156	10					2496	0.4283	0.32	0.05785	0.28	0.94	0.053670	0.11	362.5	361.8	357.0
	250-150Lh	5.400	139	9					3710	0.4301	0.29	0.05799	0.28	0.95	0.053790	0.09	363.4	363.3	362.0
	<74um	3.800	210	13					5551	0.4329	0.29	0.05830	0.28	0.97	0.053860	0.07	365.3	365.3	365.0
	200um, Ab48*	1 grain	162	11					1757	0.4275	0.46	0.05764	0.35	0.77	0.053781	0.29	361.3	361.4	362.0
	200um, Ab6*	1 grain	154	10					1917	0.4275	0.52	0.05763	0.40	0.79	0.053805	0.32	361.2	361.4	363.0
	200um, Lh28*	1 grain	288	19					1064	0.4261	0.58	0.05741	0.41	0.77	0.053825	0.38	359.9	360.4	364.0
	200um*	1 grain	140	9					1341	0.4215	0.27	0.05699	0.24	0.89	0.053647	0.11	357.3	357.2	356.0
Riwaka	z1a AnLh**	0.009	60	4	0.4	83.7	0.92	0.294	4565	0.4287	0.17	0.05774	0.15	0.86	0.053853	0.09	361.8	362.3	365.0
P71392	z2a AnLh**	0.011	35	2	0.4	73.6	0.83	0.266	4105	0.4289	0.38	0.05774	0.25	0.67	0.053879	0.28	361.9	362.4	366.0
	z3 AnLh**	0.007	68	5	0.5	59.7	0.90	0.287	3280	0.4309	0.13	0.05798	0.08	0.63	0.053894	0.11	363.3	363.8	366.7
	z4, AnLh**	0.009	91	6	0.3	193.9	1.03	0.325	10314	0.4315	0.08	0.05807	0.05	0.64	0.053886	0.06	363.9	364.2	366.3
	z5 AnLh**	0.014	62	4	0.4	152.9	0.93	0.295	8322	0.4322	0.09	0.05817	0.06	0.66	0.053883	0.07	364.5	364.7	366.2
	z6 Ab, AnLh**	0.007	111	7	0.6	78.1	0.63	0.201	4582	0.4312	0.10	0.05803	0.06	0.65	0.053885	0.08	363.7	364.0	366.2
	z7 Ab, AnLh**	0.008	88	6	0.7	68.8	0.93	0.295	3753	0.4312	0.10	0.05804	0.07	0.68	0.053885	0.08	363.7	364.1	366.2
	z8 Ab, AnLh**	0.012	65	4	0.6	89.2	0.76	0.240	5068	0.4315	0.10	0.05808	0.06	0.62	0.053890	0.08	363.9	364.3	366.4
	z9**	0.005	85	6	1.9	14.8	1.01	0.323	824	0.4259	0.35	0.05735	0.25	0.75	0.053864	0.23	359.5	360.3	365.4
Foulwind	mz1,360x240x180um**	0.033	2241	440	36.1	405.4	10.72	3.402	6657	0.3697	0.08	0.05077	0.07	0.83	0.052811	0.05	319.2	319.4	320.7
OU49201	mz2, 180x130x65um**	0.004	837	342	4.5	289.5	26.75	8.490	2262	0.3586	0.28	0.04943	0.18	0.65	0.052618	0.21	311.0	311.2	312.3
	z2(3) Ab**	0.002	490	24	2.9	13.3	0.24	0.076	900	0.3671	0.29	0.05049	0.23	0.84	0.052732	0.16	317.5	317.5	317.3
	z3 Ab**	0.001	664	32	0.7	23.4	0.13	0.043	1620	0.3699	0.25	0.05080	0.14	0.61	0.052806	0.20	319.5	319.6	320.5
	z4 Ab**	0.001	236	12	0.6	13.2	0.25	0.081	889	0.3648	0.38	0.05007	0.23	0.65	0.052841	0.29	315.0	315.8	321.9
	cg	8.200	570	36					3640	0.5675	0.37	0.06453	0.30	0.85	0.063780	0.19	403.1	456.4	734.5

Table DR1. U-Pb data for Paleozoic plutons of western New Zealand and West Antarctica

Crosscut	z1 Ab**	0.0063	241.71	14	1.0	86.8	0.19	0.082	5719	0.4826	0.14	0.06065	0.09	0.68	0.057713	0.10	379.55	399.84	518.91
P52241	z2 Ab **	0.0051	331.92	19	2.7	35.1	0.18	0.058	2383	0.4381	0.19	0.05888	0.12	0.64	0.053971	0.15	368.78	368.93	369.82
	z3 Ab**	0.009	393	22	1.2	157.0	0.16	0.051	10659	0.4374	0.08	0.05881	0.05	0.65	0.053939	0.06	368.4	368.4	368.5
	mz	0.100	2502	1987					750	0.4297	1.27	0.05817	1.24	0.98	0.053583	0.25	364.5	363.0	353.6
	mz	0.300	789	643					572	0.4109	0.98	0.05559	0.46	0.95	0.053616	0.86	348.7	349.6	354.9
Tarn Summit	z1 Ab**	0.008	473	26	1.0	217.8	0.12	0.039	14936	0.4459	0.08	0.05954	0.06	0.75	0.054315	0.05	372.8	374.4	384.1
OU49209	z2 Ab**	0.009	490.69	27	0.8	320.3	0.14	0.044	21860	0.4398	0.08	0.05906	0.05	0.65	0.054013	0.06	369.91	370.14	371.57
	z3 Ab**	0.0017	405.49	23	0.8	464.6	0.14	0.045	31675	0.4393	0.07	0.05901	0.04	0.67	0.053997	0.05	369.58	369.77	370.91
	>74um Lh	0.900	777	45					13794	0.4406	0.28	0.05913	0.27	0.98	0.054048	0.05	370.3	370.7	373.0
	mz fg	1.200	2740	959					6143	0.4063	1.29	0.05540	1.28	0.99	0.053188	0.13	347.6	346.2	336.8
Maruia	180um, ar 5:1**Ab	0.006	661	36	1.80			0.05	7596	0.4056	0.11	0.05502	0.08	0.71	0.053470	0.08	345.3	345.7	348.8
P52247																			
Tobin	~300um Ab24*	0.100	443	30					378	0.4067	0.39	0.05512	0.33	0.87	0.053510	0.20	345.9	346.5	350.5
P61003	175-150, 5:1, Lh 8 gr*	0.200	342	20					10230	0.4040	0.18	0.05478	0.16	0.92	0.053504	0.07	343.7	344.5	350.2
	250, 5:1, Lh 5 gr*	0.110	541	32					8982	0.4039	0.20	0.05479	0.18	0.92	0.053476	0.08	343.8	344.5	349.1
	600um prism, Ab6*	0.080	513	30					5231	0.4043	0.83	0.05493	0.82	0.99	0.053387	0.11	344.7	344.8	345.3
Barrytown	z1 Ab**	0.005	384	21.8	1.2	97.1	0.27	0.088	6380	0.4315	0.08	0.05793	0.06	0.68	0.054028	0.06	363.01	364.26	372.2
P45412	z2 AnLh**				0.3	74.39	0.32	0.102	4737	0.4407	0.17	0.05907	0.08	0.49	0.054114	0.15	369.95	370.76	375.8
	z3 AnLh**				0.3	170.6	0.30	0.096	10896	0.4380	0.11	0.05880	0.06	0.56	0.054018	0.10	368.35	368.82	371.8
	z4 AnLh**				0.3	269.0	0.62	0.196	15785	0.4373	0.07	0.05879	0.05	0.65	0.053944	0.06	368.28	368.34	368.7
	z5 AnLh**				0.8	95.3	0.19	0.059	6303	0.4370	0.11	0.05878	(.06)	0.55	0.053920	0.09	368.21	368.14	367.7
	mz cg	0.015	3952	1600					3112	0.4354	0.99	0.05882	0.98	0.99	0.053687	0.12	368.5	367.0	357.9
	74-105	1.000	469	39					1811	0.7988	0.29	0.08060	0.27	0.95	0.071874	0.09	499.7	596.1	982.4
Falls Ck	mz1	0.600	1956	640					2211	0.4507	0.22	0.06054	0.20	0.95	0.053996	0.09	378.9	377.5	370.9
P45587	mz2	0.220	2632	866					3386	0.4470	0.76	0.06030	0.75	0.99	0.053762	0.11	377.5	375.2	361.1
	<44um Lh	1.600	397	25					6161	0.4531	0.28	0.06012	0.27	0.98	0.054663	0.06	376.3	379.5	398.5
	>74um Lh	3.500	277	19					18551	0.5600	0.28	0.06650	0.27	0.98	0.061069	0.05	415.0	451.5	641.7
Rangitoto*	z1 Ab**	0.0015	627	37	0.6	103.44	0.31	0.098	6601	0.4380	0.11	0.05883	0.07	0.623	0.053995	0.09	368.50	368.82	370.8
P52355	z2 Ab**	0.0019	331	20	0.5	77.3	0.42	0.132	4800	0.4385	0.14	0.05894	0.09	0.683	0.053961	0.10	369.18	369.21	369.4
	z3 Ab**	0.0021	539	32	0.7	92.7	0.31	0.097	5922	0.4378	0.12	0.05883	0.08	0.662	0.053972	0.09	368.50	368.69	369.9
	z4 AnLh**				0.4	66.8	0.56	0.176	4000	0.4400	0.18	0.05907	0.08	0.467	0.054023	0.16	369.98	370.26	372.0
	z5 AnLh**				0.4	182.1	0.44	0.138	11215	0.4392	0.10	0.05901	0.06	0.564	0.053984	0.09	369.58	369.69	370.4
	z6 AnLh**				0.4	137.5	0.42	0.132	8519	0.4397	0.11	0.05908	0.05	0.513	0.053976	0.09	370.02	370.02	370.1
	z7 AnLh**				1.0	22.4	0.40	0.129	1408	0.4413	0.26	0.05914	0.15	0.601	0.054118	0.21	370.38	371.15	375.9
Kakapotahi*	mz	1.800	3666	1143					25777	0.4507	1.12	0.06068	1.12	0.99	0.053867	0.08	379.8	377.8	365.5
P52283	mz	0.300	3422	1173					493	0.4462	0.91	0.06014	0.82	0.91	0.053808	0.39	376.5	374.6	363.0
Paringa	z1 Ab**	0.002	449	28	1.0	60.9	0.54	0.170	3662	0.4382	0.12	0.05890	0.07	0.603	0.053958	0.10	368.91	368.96	369.3
P45595	z2 AnLh**				0.5	63.6	0.41	0.130	3957	0.4389	0.15	0.05894	0.07	0.514	0.054010	0.13	369.16	369.48	371.5
	z3 AnLh**				0.4	68.2	0.35	0.111	4311	0.4399	0.13	0.05901	0.07	0.569	0.054064	0.11	369.61	370.17	373.7
	z4 AnLh**				0.5	98.4	0.78	0.248	5555	0.4394	0.22	0.05897	0.14	0.656	0.054045	0.17	369.37	369.86	373.0
	z5 AnLh**				0.6	80.1	0.42	0.134	4960	0.4400	0.17	0.05897	0.08	0.467	0.054113	0.15	369.35	370.23	375.7
	z6 AnLh**				0.5	63.43	0.43	0.137	3924	0.4399	0.14	0.05900	0.08	0.556	0.054078	0.12	369.51	370.17	374.3
	Titanite*	8.000	12.434	1.276					211	0.4329	0.90	0.05823	0.40	0.49	0.053924	0.79	364.8	365.3	367.9
Fiordland block																			

Table DR1. U-Pb data for Paleozoic plutons of western New Zealand and West Antarctica

Horatio	350x75um, 1gr, Ab**	0.006	358	20	2.3	51.5	0.41	0.130	3207.6	0.4126	0.13	0.05587	0.09	0.68	0.053560	0.10	350.48	350.75	352.6
OU49111	300x60um, 3gr, Ab**	0.010	415	24	1.1	223.5	0.43	0.138	13777	0.4094	0.13	0.05543	0.06	0.46	0.053574	0.12	347.75	348.46	353.2
Dolphin	cg Lh	5.700	180	10					39631	0.4290	0.28	0.05779	0.28	0.98	0.053839	0.05	362.2	362.5	364.3
OU49115	Kfg	21.200	299	17					5476	0.4290	0.33	0.05773	0.33	0.98	0.053902	0.07	361.8	362.5	367.0
	Kcg	20.020	171	11					484	0.4261	0.56	0.05750	0.32	0.96	0.053740	0.44	360.4	360.4	360.0
Mt Evans	z1 Ab**	0.006	198	11	0.6	110.6	0.23	0.072	7368	0.4115	0.08	0.05575	0.05	0.66	0.053539	0.06	349.7	350.0	351.7
P78948	z2 Ab**	0.005	229	13	0.4	132.1	0.34	0.106	8537	0.4109	0.10	0.05572	0.06	0.60	0.053485	0.08	349.5	349.5	349.4
	<105um Ab	3.60	513	36					27241	0.6206	0.28	0.07156	0.28	0.98	0.062895	0.06	445.6	490.2	704.7
Newton	z2 Ab**	3.7	362	19	0.5	153.2	0.13	0.043	10479	0.4078	0.08	0.05529	0.05	0.64	0.053500	0.06	346.9	347.3	350.1
P64999	z1 Ab**	2.9	903	47	1.0	135.9	0.15	0.048	9252	0.4038	0.08	0.05479	0.05	0.64	0.053461	0.06	343.8	344.4	348.4
Houseroof	mz 1	2.00	613.67	338				0.0986	1646	0.4106	0.54	0.05606	0.52	0.96	0.053129	0.16	351.6	349.33	334.3
OU58013	mz 3	0.50	2011.6	1105				0.0971	2118	0.404	1.33	0.05531	1.32	0.99	0.052982	0.17	347.0	344.6	328.0
Tower	z1 AnLh**				0.6	63.5	0.49	0.154	3874	0.4126	0.14	0.05592	0.07	0.53	0.053517	0.12	350.8	350.8	350.8
P73425																			
Poteriteri	z1 AnLh**				0.4	112	0.60	0.190	6600.7	0.3843	0.13	0.052480	0.07	0.567	0.053107	0.11	329.73	330.18	333.3
P74751	z2 AnLh**				0.4	127	0.46	0.146	7811.9	0.3835	0.10	0.052412	0.06	0.588	0.053072	0.08	329.31	329.63	331.8
	z3 AnLh**				0.4	237	0.43	0.138	14578.2	0.3832	0.08	0.052387	0.05	0.633	0.053047	0.06	329.16	329.36	330.8
Alice	z2 AnLh**				0.5	21.2	0.77	0.244	1216.8	0.3996	0.35	0.054325	0.17	0.555	0.053350	0.29	341.02	341.37	343.7
P74756	z1 AnLh**				0.4	30.3	0.82	0.258	1710.0	0.3986	0.29	0.054314	0.13	0.530	0.053224	0.24	340.95	340.62	338.4
	z3 AnLh**				0.5	51.3	0.77	0.245	2915.5	0.3991	0.18	0.054292	0.09	0.538	0.053309	0.15	340.82	340.97	342.0
Big	z1 AnLh**				0.3	199.3	0.49	0.156	12093	0.4181	0.09	0.05649	0.05	0.64	0.053679	0.07	354.21	354.66	357.6
P70787	z2 AnLh**				1.4	72.7	0.23	0.072	4752	0.4179	0.09	0.05650	0.06	0.69	0.053643	0.06	354.28	354.52	356.1
	z3 AnLh**				0.3	225.0	0.47	0.149	13735	0.4182	0.08	0.05651	0.05	0.58	0.053667	0.07	354.39	354.75	357.1
	z4 AnLh**				0.3	322.7	0.30	0.094	20638	0.4182	0.09	0.05657	0.05	0.58	0.053618	0.07	354.75	354.79	355.0
	z5 AnLh**				0.7	49.3	0.34	0.108	3131	0.4181	0.12	0.05654	0.07	0.61	0.053627	0.10	354.57	354.68	355.4
	z6 AnLh**				0.4	123.1	0.22	0.071	8053	0.4177	0.10	0.05651	0.05	0.53	0.053607	0.08	354.35	354.38	354.6
Ridge dike	z1 AnLh**				0.4	330.1	1.23	0.391	16745	0.4121	(.08)	0.05582	(.05)	0.593	0.053544	0.07	350.1	350.4	352.0
P71266	z2 AnLh**				0.5	221.7	0.36	0.113	13960	0.4130	(.09)	0.05600	(.05)	0.571	0.053488	0.07	351.2	351.0	349.6
Stewart Island																			
Ruggedy	220x90, Ab**	0.003	255	15	4.0	12.1	0.52	0.164	763	0.3996	0.63	0.05441	0.57	0.92	0.053260	0.25	341.6	341.4	340.1
P 62175	200x80, Ab**	0.003	279	17	5.7	8.9	0.50	0.158	566	0.4016	0.61	0.05461	0.53	0.89	0.053340	0.27	342.8	342.8	343.4
Freds Camp	z1 AnLh**				0.4	60.3	0.57	0.181	3598	0.3515	(.16)	0.04858	(.08)	0.543	0.052472	0.14	305.83	305.85	306.0
P 57426	z2 AnLh**				0.6	66.2	0.57	0.182	3949	0.3513	(.15)	0.04854	(.07)	0.495	0.052490	0.13	305.55	305.70	306.8
	z3 AnLh**				0.4	80.7	0.55	0.176	4835	0.3515	(.14)	0.04857	(.07)	0.517	0.052491	0.12	305.76	305.88	306.9
	z4 AnLh**				1.1	33.8	0.62	0.196	2000	0.3516	(.17)	0.04855	(.10)	0.654	0.052525	0.13	305.61	305.93	308.3
P 58515	150-125, 3 gr*	0.02	663	27					895	0.2428	0.48	0.03354	0.39	0.82	0.052508	0.30	212.7	220.7	307.6
Ridge	z1 Ab**	0.002	155.3	10.6	0.5	31.3	0.28	0.114	1976	0.5418	0.21	0.06746	0.15	0.74	0.058249	0.15	420.8	439.6	539.2
P 57323	z2 Ab**	0.001	152.2	9.7	6.0	27.6	0.63	0.158	1617	0.4403	0.46	0.05866	0.25	0.58	0.054441	0.38	367.5	370.5	389.3
	z3 Ab**	0.001	241.5	14.7	0.5			0.211	210	0.4679	2.45	0.05684	2.33	0.96	0.059701	0.65	356.4	389.7	592.7
	z4 AnLh**				0.3	208.1	0.11	0.049	13627	1.1158	0.08	0.11178	0.05	0.59	0.072393	0.07	683.1	761.0	997.0
	z5 AnLh**				0.2	48.9	0.40	0.129	3049	0.4128	0.15	0.05584	0.08	0.54	0.053621	0.13	350.3	350.9	355.2
	100-75 lh*	0.10	152	9					760	0.4030	0.36	0.05477	0.27	0.76	0.053361	0.24	343.7	343.8	344.1
Table	z2 Ab**	0.002	654.4	39.5	0.4	92.7	0.32	0.290	9396	0.3829	0.09	0.05224	0.05	0.62	0.053161	0.07	328.2	329.2	335.7
P60678	z1 Ab**	0.001	998.8	45.3	0.7	172.2	0.89	0.113	5788	0.3290	0.10	0.04525	0.06	0.62	0.052728	0.08	285.3	288.8	317.1
Knob	mz 125x90x40,15 gr*	0.09	750	30					6245	0.3215	0.78	0.04444	0.77	0.99	0.052460	0.90	280.2	283.1	305.5

Table DR1. U-Pb data for Paleozoic plutons of western New Zealand and West Antarctica

P63648	mz 315x200x?, 1 gr*	0.10	1695	622	3170	0.3092	0.44	0.04277	0.44	0.98	0.052443	0.62	269.9	273.6	304.8
Marie Byrd Land															
Chester Mts	mz fg	4.00	3049	712	2044	0.4114	0.34	0.05585	0.31	0.92	0.053431	0.13	350.3	349.9	347.2
Chester2	mz cg	4.00	2501	657	3332	0.4242	0.44	0.05746	0.43	0.98	0.053551	0.08	360.2	359.1	352.2
Neptune	mz fg	2.60	7498	911	7630	0.4026	0.22	0.05468	0.21	0.97	0.053400	0.05	343.2	343.6	345.8
Neptune6	mz cg	3.00	6354	856	5834	0.3961	0.27	0.05388	0.26	0.98	0.053321	0.05	338.3	338.8	342.5

Mineral analysed is zircon, unless noted: mz is monazite. Ab is air abrasion, Lh is leaching AnLh is Annealing and Leaching pretreatment (Mattinson 2003).
San Diego State University
Samples: prefix OU Geology Department at Otago University followed by NZMS grid reference.
Fractions analyzed; 60, 100, 200 = mesh sizes; cg = coarse grained, bulk. L indicates leaching of fraction with HF on hotplate at c.100°C for 2 days prior to dissolution following methods outlined in Kimbrough et al. (1992).
Separation of U and Pb was done using HCl column chemistry. Concentrations were determined using a mixed 208Pb/235U spike.
Lead isotopic compositions corrected for ~0.10% ±0.05% per mass unit mass fractionation, based on replicate analyses of NBS 981 & NBS 983. Errors for 206Pb/204Pb measurements were minimized by use of an ion counting Daly multiplier system for detection of the small 204Pb signal and are typically less than 1%.
Ages calculated with following decay constants: 1.55125E-10 = 238U and 9.8485E-10 = 235U. Present day 238U/235U = 137.88.
Corrections for common lead were made using Stacey and Kramers (1975) lead model isotopic compositions for the interpreted crystallization age. Total lead blanks averaged c. 25 picograms. Pb* = radiogenic lead. The 2-sigma value for analytical errors are shown in parentheses behind lead isotopic compositions.
Accuracy of 206*Pb/238U dates is better than ±0.5% (c. ˜±1Ma) based on long-term reproducibility of a "standard" zircon sample (OU49127). Uncertainties in the 207*Pb/206*Pb dates computed with PBDAT (Ludwig, 1989) and are stated at the two-sigma level assuming a ±0.1 uncertainty in the common 207Pb/204Pb.

*GNS Science /Otago University/Brown University (NW Walker)
? Size of longest dimension in microns; ab = mechanically abraded for 6 hours; L = 24 hr leach in 48%HF on hotplate in sealed Teflon capsule prior to digestion.
+Total Pb concentration includes blank Pb, common Pb in zircon and radiogenic Pb. Total procedural blanks are ~2 picograms for U and ~8 picograms forPb.
Measured isotopic ratios corrected for mass fractionationof ~ 0.11% per atomic mass unit based on analyses of NIST SRM981 and 982 and adjusted for small amount of 206Pb in tracer.
Uncertainty in the calculated ages is stated at the two-sigma level and estimated from combineduncertainties in calibrations of mixed 205Pb - 233U - 235U tracer, measurement of isotopic ratios of Pb and U, common and laboratory blank Pb isotopic ratios, Pb and U mass fractionation corrections, and reproducibility in measurement of NIST Pb and U standards.

**MIT
Sample weights are estimated by using a video monitor and are known to within 40%. Corr. coef. = correlation coefficient.
206Pb/204Pb -measured ratio corrected for spike and fractionation only. # Corrected for fractionation, spike, blank, and initial common Pb.
Mass fractionation correction of 0.25%/amu ± 0.04%/amu (atomic mass unit) was applied to single-collector Daly analyses and 0.07%/amu ± 0.04% for dynamic Faraday-Daly analyses. Total procedural blank less than 0.5 pg for Pb and less than 0.1 pg for U. c is common Pb, rad is radiogenic Pb
Blank isotopic composition: 206Pb/204Pb = 19.10 ± 0.1, 207Pb/204Pb =15.71 ± 0.1, 208Pb/204Pb = 38.65 ± 0.1.
Age calculations are based on the decay constants of Steiger and Jäger (1977). Common-Pb corrections were calculated by using the model of Stacey and Kramers (1975) and the interpreted age of the sample.

Table S2. Sr, Nd isotopic data for Paleozoic plutons of western New Zealand

Sample no.	Pluton/unit	Granite type	Age, Ma	Rb ppm	Sr ppm	87Rb/86Sr	87Sr/86Sr	err	Sri	Sm ppm	Nd ppm	147Sm/144Nd	143Nd/144Nd	err	eNd (T)	TDM
Buller																
P45423*	Flanagan	I	350	43.9	332.7	0.38	0.706531	15	**0.70464**	2.9	11.6	0.148	0.512419	10	**-2.1**	1.7
P50892	Toropuihi-1	A	300	512.0	15.39	101	1.1616	1	**?**	9.6	29.2	0.2005	0.512751	4	**2.1**	
OU49201	Foulwind	A	320	223.8	115	5.646	0.737013	13	**0.71130**	13.1	66.2	0.1194	0.512475	4	**0.1**	0.9
P45613	Barrytown rim	S	368	239.8	108.1	6.516	0.746507	12	**0.71237**	8.2	41.9	0.1185	0.512185	20	**-5.0**	1.4
UC6762	Barrytown core	S	368	310.6	69.8	12.953	0.776073	9	**0.70821**	10.4	50.4	0.1246	0.512147	5	**-6.1**	1.5
OU45278*	Tobin	I	350	51.6	336.8	0.44	0.707115	15	**0.70492**	8.0	37.2	0.1300	0.512483	10	**0.0**	1.2
P45595	Paringa	I	368	50.5	485.6	0.301	0.708362	10	**0.70678**	2.6	15.2	0.1069	0.512307	4	**-2.1**	
P52247	Maruia	S	350	131.0	274	1.384	0.71330	14	**0.70640**	na	na	na	na	na	**na**	
P78948**	Mt Evans	S	350	154.5	135.1	3.318	0.72602	4	**0.70949**	5.4	26.3	0.1251	0.512208	20	**-5.2**	1.6
P40732**	Greenland Gp		360	124.0	98.6	3.653	0.738570	40	**0.71985**	6.2	32.1	0.1168	0.511892	20	**-10.9**	2.0
P39122**	Greenland Gp		360	111.5	159.3	2.031	0.730010	40	**0.71960**	6.7	34.0	0.1185	0.512027	20	**-8.3**	1.8
Takaka																
P51535	Motueka-1	A	350	148.6	163.8	0.0725	0.718847	11	**0.70575**	4.4	14.7	0.1334	0.512752	12	**5.1**	
OU49115	Dolphin	I	360	2.9	781.6	0.1114	0.704293	12	**0.70375**	3.1	15.1	0.1248	0.512652	8	**3.6**	
P57098	Milford	I	360	42.2	591.9	0.2059	0.704505	9	**0.70345**	3.9	18.7	0.1251	0.512601	4	**2.6**	
OU51818***	George Sound	A	300	87.4	233.7	1.083	0.71006	30	**0.70544**	5.1	34.1	0.0903	0.512411	9	**0.3**	
OU51820***	George Sound	A	300	14.0	663.1	0.0612	0.705411	36	**0.70515**	9.0	46.1	0.1185	0.512610	21	**3.0**	
OU51828***	George Sound	A	300	129.5	120.3	3.118	0.721921	19	**0.70861**	12.2	49.8	0.1481	0.512663	20	**2.7**	
OU51833***	George Sound	A	300	81.6	454.7	0.5193	0.707464	38	**0.70525**	14.7	89.3	0.0998	0.512623	16	**4.0**	
OU51833***	George Sound	A	300	32.9	922.8	0.103	0.704481	19	**0.70404**	8.3	36.8	0.1369	0.512733	15	**4.5**	
OU51837***	George Sound	A	300	95.4	51.95	5.338	0.750917	21	**0.72813**	20.6	77.3	0.1612	0.512669	12	**2.2**	
P57323	Ridge	S	345	103.7	408.9	7.522	0.71064	12	**0.70704**	4.8	25.3	0.1147	0.512175	5	**-5.4**	1.3
OU49111**	Horatio	S	350	41	339.2	0.3502	0.70762	4	**0.70587**	4.1	22.6	0.1084	0.512322	20	**-2.2**	1.2
P57426	Freds Camp	Peralk	300	285.9	13.1	64.41	0.859232		**?**	5.9	30.0	0.1192	0.512858	5	**1.9**	
P58515	Freds Camp	Peralk	300	64.0	79	2.430	0.716355	20	**0.70598**	2.5	11.5	0.1335	0.512538	5	**0.6**	
P63648**	Knob	A	310	182.6	129.8	4.083	0.72639	36	**0.70838**	10.9	60.6	0.1086	0.512305	20	**-3.0**	
P62175	Ruggedy	I	340	96.2	72.5	3.770	0.720528	11	**0.70228**	5.3	24.6	0.1307	0.512581	6	**1.9**	
OU49156	Echinus	I	310	55.1	205	0.763	0.706475	12	**0.70311**	3.1	15.4	0.1223	0.512600	17	**2.2**	
OU49141*	Roxburgh	I	340	10.1	169.4	0.17	0.706158	15	**0.70533**	4.3	27.5	0.0950	0.512447	10	**0.7**	0.9

Samples analysed by N.Walker, Brown University, except where otherwise indicated
* Analysed by D.L.Parkinson at UCSB:
Sr normalized to 86Sr/88Sr = 0.1194; NBS 987 = 0.710235, BCR-1 = 0.70500. T DM calculated using 143Nd/144Nd(0)=0.51315; 147Sm/144Nd=0.2137;
present day CHUR=0.512638, with 146Nd/144Nd=0.7219. Ames=0.511890 ± 10 (n>25); BCR-1=0,512630 ± 10 (n=10)
** Analysed at La Trobe University (Roland Maas) May, June 2001
All Nd isotope ratios are relative to LaJolla=0.511860. CHUR is 0.512638. Depleted mantle model ages calculated for linear depleted mantle
evolution (4.57 Ga to 0 Ga) with present-day parameters of 0.2136 and 0.513144
Errors (2 sigma pop) based on reproducibility of standard rocks: 87Rb/86Sr ±0.5%; 87Sr/86Sr ±0.00004 or about ±0.006%
147Sm/144Nd ±0.2%; 143Nd/144Nd ±0.000020 or ±0.004%. In-run errors are always less than quoted reproducibilites
*** Analysed by DLK, San Diego State University   na not analysed

Table DR3. Oxygen isotope data for quartz from Paleozoic plutons

	Granite type	Sample	$\delta^{18}O$ Qtz	$\delta^{18}O$ magma
Karamea				
Oparara	S	P45397	12.5	11.0
Waterfall	S	OU50115	13.5	12.0
Dunphy	S	P45395	12.9	11.4
Dunphy	S	RNZ199	14.4	12.9
Dunphy	S	RNZ212	14.4	12.9
Whale Ck	S	P45394	12.8	11.3
Whale Ck	S	RNZ169	12.6	11.1
O'Sullivans	S	RNZ120	13.4	11.9
Barrytown	S	KF190201-10	12.9	11.4
Barrytown	S	P45613	13.5	12.0
Tarn Summ	S	OU49209	12.5	11.0
Tarn Summ	S	R6156	12.6,12.7	11.2
Crosscut	S	P52241	12.2, 12.3	10.8
Falls Creek	S	P45587	14.0	12.5
Kakapotahi	S	P52283	12.2	10.7
Mt. Evans	S	P78948	12.5	11.0
Paringa				
Domett	I	P45425	10.5, 10.6	9.0
Paringa	I	P45595	10.1, 10.3	8.7
Riwaka	I	P46105	10.6, 10.7	9.1
Ridge				
Maruia	S	P52247	11.8	10.3
Horatio	S	OU49111	11.7, 11.8	10.3
Ridge	S	P57323	12.3	10.8
Tobin				
Tobin	I	P61003	12.3, 12.5	10.9
Tobin	I	OU45278	12.1, 12.2	10.7
Flanagan	I	P45423	8.6	7.1
Ruggedy	I	P62175	6.5	5.0
Ruggedy	I	OU56533	6.6	5.1
L Roxburgh	I	OU49141	7.2	5.7
Foulwind				
Foulwind	A	OU49201	12.4, 12.8, 12.7	11.2
Foulwind	A	P52256	12.8, 13.0	11.4
Knob	A	P63648	8.4, 8.5 (zrn)	9.6
Toropuihi-1	A	P50892	7.5	6.0
Greenland Group, Buller Terrane (whole rock)				
		S44/p112A	15.5	
		S44/p86	15.9	
		P40732	15.8	
		P30816	13.7	
		P39122	16.2	

Table S4. Chemical analyses of granites from Marie Byrd Land

(wt %) XRF	Chester 2	Neptune 6
	2-mica granite	2-mica granite
SiO2	74.15	75.85
TiO2	0.207	0.109
Al2O3	14.43	13.17
Fe2O3*	1.49	1.28
MnO	0.036	0.033
MgO	0.28	0.16
CaO	0.93	0.89
Na2O	3.24	3.26
K2O	4.98	4.47
P2O5	0.186	0.198
LOI		
Total	99.93	99.42
(ppm) XRF		
Ni	13	10
Cr	6	3
Sc	1	4
V	12	0
Ba	149	82
Rb	338	241
Sr	67	53
Zr	94	66
Y	23	22
Nb	16.3	13.2
Ga	22	18
Cu	2	2
Zn	47	36
Pb	32	35
La	0	24
Ce	60	36
Th	16	9
ICP-MS:		
La	23.52	14.27
Ce	47.86	28.58
Pr	5.36	3.17
Nd	20.68	11.93
Sm	4.41	3.52
Eu	0.55	0.37
Gd	4.09	3.29
Tb	0.69	0.67
Dy	4.04	3.83
Ho	0.77	0.68
Er	2.12	1.83
Tm	0.31	0.26
Yb	1.89	1.63
Lu	0.29	0.25
Ba	180.00	96.00
Th	11.71	8.68
Nb	16.87	20.09
Y	22.96	21.46
Hf	2.92	2.06
Ta	1.93	3.45
U	1.47	5.63
Pb	32.04	35.20
Rb	337.75	239.35
Cs	12.28	10.43

Analyses performed at the GeoAnalytical Laboratory, Washington State University